



AFRL-AFOSR-UK-TR-2019-0049

Joint Physics Initiative for study of orbital angular momentum mode
fiber amplification of optical pulses

Johan Nilsson
UNIVERSITY OF SOUTHAMPTON
UNIVERSITY RD
SOUTHAMPTON, SO17 1BJ
GB

09/12/2019
Final Report

DISTRIBUTION A: Distribution approved for public release.

Air Force Research Laboratory
Air Force Office of Scientific Research
European Office of Aerospace Research and Development
Unit 4515 Box 14, APO AE 09421

REPORT DOCUMENTATION PAGE				Form Approved OMB No. 0704-0188	
<p>The public reporting burden for this collection of information is estimated to average 1 hour per response, including the time for reviewing instructions, searching existing data sources, gathering and maintaining the data needed, and completing and reviewing the collection of information. Send comments regarding this burden estimate or any other aspect of this collection of information, including suggestions for reducing the burden, to Department of Defense, Executive Services, Directorate (0704-0188). Respondents should be aware that notwithstanding any other provision of law, no person shall be subject to any penalty for failing to comply with a collection of information if it does not display a currently valid OMB control number.</p> <p>PLEASE DO NOT RETURN YOUR FORM TO THE ABOVE ORGANIZATION.</p>					
1. REPORT DATE (DD-MM-YYYY) 12-09-2019		2. REPORT TYPE Final		3. DATES COVERED (From - To) 24 Sep 2016 to 23 Sep 2018	
4. TITLE AND SUBTITLE Joint Physics Initiative for study of orbital angular momentum mode fiber amplification of optical pulses				5a. CONTRACT NUMBER	
				5b. GRANT NUMBER FA2386-16-1-0005	
				5c. PROGRAM ELEMENT NUMBER 61102F	
6. AUTHOR(S) Johan Nilsson, Balaji Srinivasan, Siddharth Ramachandran				5d. PROJECT NUMBER	
				5e. TASK NUMBER	
				5f. WORK UNIT NUMBER	
7. PERFORMING ORGANIZATION NAME(S) AND ADDRESS(ES) UNIVERSITY OF SOUTHAMPTON UNIVERSITY RD SOUTHAMPTON, SO17 1BJ GB				8. PERFORMING ORGANIZATION REPORT NUMBER	
9. SPONSORING/MONITORING AGENCY NAME(S) AND ADDRESS(ES) EOARD Unit 4515 APO AE 09421-4515				10. SPONSOR/MONITOR'S ACRONYM(S) AFRL/AFOSR IOE	
				11. SPONSOR/MONITOR'S REPORT NUMBER(S) AFRL-AFOSR-UK-TR-2019-0049	
12. DISTRIBUTION/AVAILABILITY STATEMENT A DISTRIBUTION UNLIMITED: PB Public Release					
13. SUPPLEMENTARY NOTES					
14. ABSTRACT <p>This report summarizes the work in a collaboration project between University of Southampton and IIT Madras on fiber amplification of pulses with orbital angular momentum (OAM). The part of the work led by IITM is reported separately. Here we focus on describing our results on Raman amplification with 15 dB gain and 20% conversion efficiency. We believe this approach is very interesting and promising, and that this is the first example of OAM mode amplification in the reported regime. On a conceptual level, we introduce the difference between local and non-local gain saturation, where Raman gain is free from local saturation. Work on simulation methods is also reported.</p>					
15. SUBJECT TERMS <p>Orbital, Angular momentum, Mode amplification, Fiber, Amplifier, Fiber Laser, Laser</p>					
16. SECURITY CLASSIFICATION OF:			17. LIMITATION OF ABSTRACT SAR	18. NUMBER OF PAGES	19a. NAME OF RESPONSIBLE PERSON LOCKWOOD, NATHANIEL
a. REPORT Unclassified	b. ABSTRACT Unclassified	c. THIS PAGE Unclassified			19b. TELEPHONE NUMBER (include area code) 011-44-1895-616005

Final report for AOARD Grant FA2386-16-1-0005

AFOSR Indo-UK-US

Joint Physics Initiative for study of orbital angular momentum mode fiber amplification of optical pulses

Date of Report: Jan 2 2019

Report Period: Sept 24 2016 – Sept 23 2018

Principal Investigator (University of Southampton)

Prof Johan Nilsson

University of Southampton

Optoelectronics Research Centre

Highfield

Southampton SO17 1BJ

United Kingdom

Office +44 23 8059 3101

jn@orc.soton.ac.uk

Co-investigators (University of Southampton, address as above)

Prof Sir David N. Payne

Office +44 23 8059 3583

dnp@orc.soton.ac.uk

Prof Jayanta K. Sahu

Office +44 23 8059 3162

jks@orc.soton.ac.uk

The contributors to the work reported here are listed in a separate section. This report was written by the following:

Johan Nilsson, Shankar Pidishety, Sheng Zhu

Abstract

This report summarizes the work in a collaboration project between University of Southampton and IIT Madras on fiber amplification of pulses with orbital angular momentum (OAM). The part of the work led by IITM is reported separately. Here we focus on describing our results on Raman amplification with 15 dB gain and 20% conversion efficiency. We believe this approach is very interesting and promising, and that this is the first example of OAM mode amplification in the reported regime. On a conceptual level, we introduce the difference between local and non-local gain saturation, where Raman gain is free from local saturation. Work on simulation methods is also reported.

Introduction

This report summarizes the work at the Optoelectronics Research Centre (ORC), University of Southampton, within the collaboration with IIT Madras (IITM, principal investigator Balaji Srinivasan, co-investigators Deepa Venkitesh and Anil Prabhakar), from Oct 2016 to Sep 2018. The work is a continuation of a previous one-year project executed under a separate grant. Thus,

Year 1: FA9550-15-1-0423 (ORC) & FA2386-15-1-5044 (IITM).

Year 2 - 3: FA2386-16-1-0005 (ORC, covered in this report) & FA2386-16-1-4077 (IITM).

The Y1 reports from ORC and IITM were essentially identical, but the present report is different from IITM's. Still, the reports remain a joint effort with contributions to both reports from both ORC and IITM.

Methods, assumptions, and procedures

At ORC we have primarily focused on building and evaluating a fiber Raman amplifier (FRA) for optical vortex beams carrying orbital angular momentum (OAM) as well as simulations on the performance of the FRA.

The objective is to improve the gain energy conversion of the FRA while preserving the mode purity of the OAM beams. Since the FRA is pumped by a multimode laser source, it can also improve the brightness.

In addition, we have fabricated a fiber and have evaluated it in a non-OAM fiber Raman laser (FRL).

On a conceptual level, we introduce the difference between local and non-local gain saturation, where Raman gain is free from local saturation. Work on simulation methods is also reported.

In addition, work on higher-order Bessel-mode amplification and suppression of stimulated Brillouin has been supported by the project. See publications for details.

Results, findings, and accomplishments

Fiber Raman amplifier for OAM beams with multimode pump

Vortex modes carrying OAM are not only immensely studied for applications in telecommunications, but are also potentially capable of scaling the effective area of a fiber mode. While OAM mode (OAMM) amplification has been demonstrated with rare-earth (RE) doped air-core fibers [1], [2], there are several effects that hamper the mode quality. Firstly, as the helical phase front of the vortex beam is highly susceptible to anisotropic perturbations, precise control of transverse and longitudinal refractive index variations is needed, which is hard for RE doped fiber. A fiber Raman amplifier, however, can utilize high quality telecom passive fibers that are widely available at low cost. On a more fundamental level, in a RE doped fiber, the donut-shaped OAMMs are prone to induce local mode-selective gain saturation, which can lead to much higher gain for unwanted modes and thus mode-purity degradation. In a FRA however, there is no such local gain saturation as the Raman gain is independent of the signal intensity. Rather, the gain saturation is a result of longitudinal pump depletion. This is a non-local effect which can only be mode-selective to the extent that the depletion alters the transverse pump intensity distribution. However, this is expected to be a much weaker effect than the local gain saturation, which

suggests that Raman amplifiers will be better for preserving the mode purity and power scaling of selected modes. Note however that buildup of power in the matched OAMM of opposite charge may be an important exception to this rule.

We have set up a fiber Raman amplifier at 1115 nm pumped by a multimode Yb doped fiber amplifier at 1060 nm. A maximum of 15 dB of average Raman gain of an OAM beam with charge 2 was achieved with $\sim 83.2\%$ mode purity. The results (including intermittent results) have been published and presented at the Laser Applications Conference 2017 (6.5 dB gain) [3] and at the Advanced Solid State Laser Conference 2018 (15 dB gain) [4] and also expanded with additional analysis and submitted to a journal [5]. Even higher gain and higher pump conversion are expected with future experiments, to the levels we have already achieved with a non-OAM higher-order mode [6], [7].

The setup for OAMM Raman amplification experiments is shown in Fig 1. A 30-m long Freelight passive fiber generates the Raman seed pulses at 1115 nm, which is then converted to charge 2 ($l = +2$, $s = +1$) OAM beam by a quarter waveplate and an S-plate [8]. The Raman gain fiber is a 5-m long few-mode passive fiber from OFS Inc. The fiber is effectively step-index with a slightly *W*-shaped refractive index profile in the center (shown in Fig. 1(b)). A 2-m long Yb doped fiber (YDF) amplifier generates the pump beam at 1060 nm.

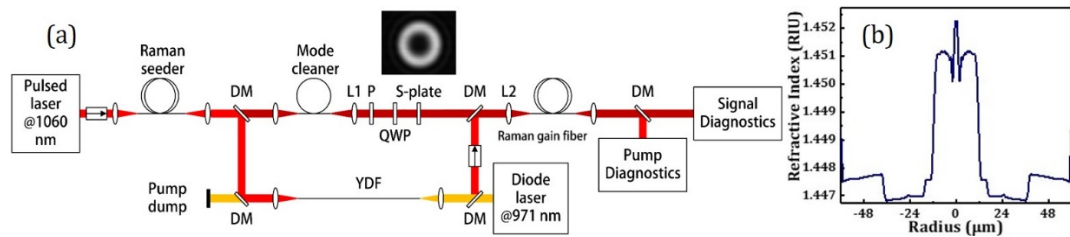


Figure 1. (a) Schematic diagram of experimental setup of Raman amplification and mode purity measurement. DM – dichroic mirror; QWP – quarter waveplate; HWP – half-waveplate; P: polarizer. Inset shows beam intensity profile after S-plate. (b) Measured refractive index profile of Raman gain fiber.

Fig. 2 shows the gain and pump depletion results and measured output spectra. The pump depletion is calculated as $(P_2 - P_1)/P_2$, where P_1 is the residual average pump power with Raman seeding and P_2 is the transmitted average pump power without Raman seeding. With launched pump pulses of 6.95 kW peak power and 382.5 μ J pulse energy, the average power Raman gain reaches maximum 15 dB. The amplified signal pulses reach 4.5 kW peak power and 68.5 μ J pulse energy. The pump depletion is 20% and pump conversion efficiency is 17.9%. The gain slope of 2.15 dB/kW corresponds to a Raman gain coefficient of 48.7 fm/W, matching the expected value for un-polarized pumping at 1060 nm. The temporal traces of incident signal pulse, incident pump pulse and transmitted signal pulse at 15 dB is shown in Fig. 2(c).

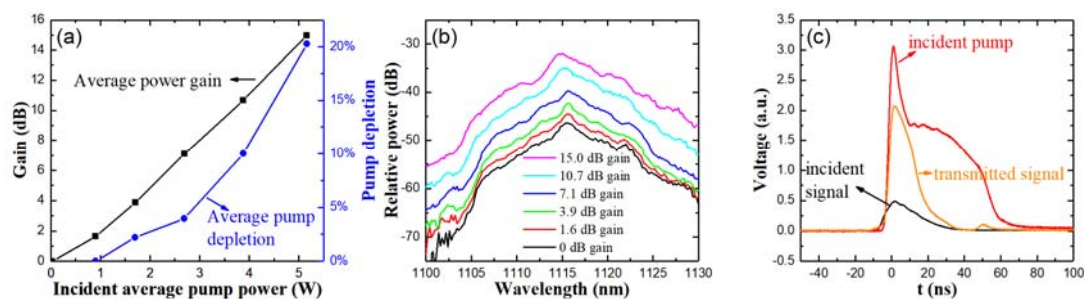


Figure 2. (a) Measured total average-power gain and pump depletion against launched pump peak power; (b) Optical spectra measured in average power with 1 nm resolution for different average-power gains; (c) Temporal traces of incident pump (red curve), incident signal (black) and transmitted signal (yellow) pulses at 15 dB Raman gain. The amplitudes of the traces have been scaled for visibility.

We have analyzed the mode purity of the amplified OAMM by decomposing the output beam into an OAM basis set with an SLM-based setup shown in Fig. 3. The output beam is converted to linear polarization parallel to the working direction of the SLM. A series of computer-generated holograms

that possess different OAM charge are displayed on the SLM and the power in the conjugate charge is approximately proportional to the on-axis intensity of the far-field diffraction pattern.

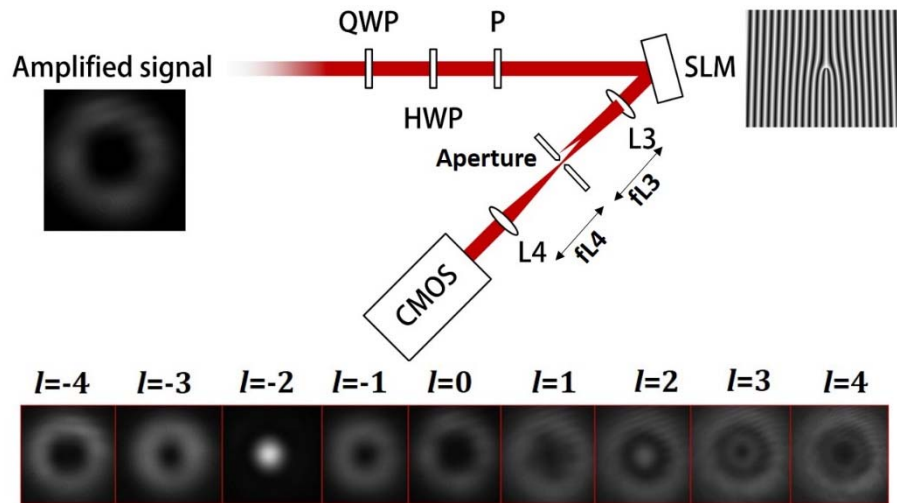


Figure 3. Schematic diagram of experimental setup for mode purity measurement. Images show beam profiles of the transmitted signal (left) and the far-field (lower-middle) of the first order diffraction from the SLM for different charge l (image brightness increased for better visibility and cropped to different scale), and a sample forked SLM pattern of $l = -2$ (right).

The measured purity of the incident and transmitted OAMM in the launched polarization ($s = +1$), without any pumping are 97.4% and 95.8% respectively. The mode purity in the other polarization is not studied as we noticed significant power is in the launched polarization in the experiment. The purity of the primary OAMM degrades to 83.2% at 15 dB gain. Fig. 4 shows the modal content of output signal beam at 0 dB and 15 dB, and the mode purity versus average signal gain. The purity degradation could be attributed to mode-selective gain saturation, mode-coupling in the fiber, and degraded launch alignment.

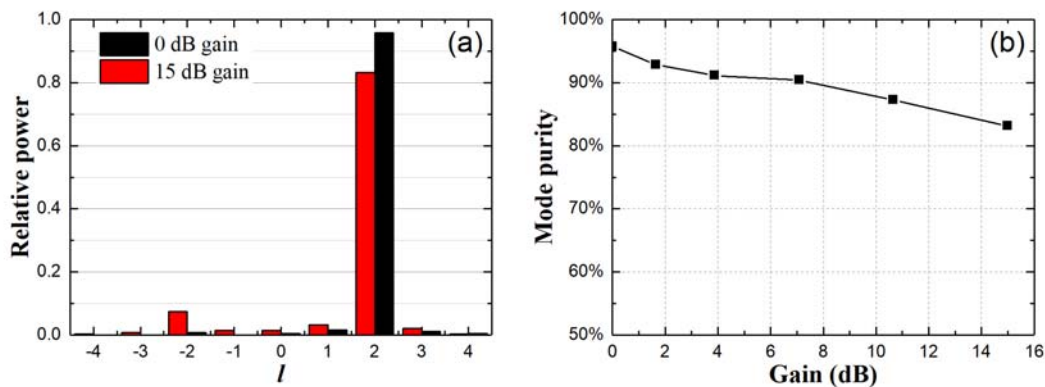


Figure 4. (a) Fraction of power in different modes vs. charge number l for 0 dB (unpumped) and 15 dB for the targeted $l=+2$ OAMM. (b) Measured mode purity for $l=+2$ OAMM versus the total average power gain.

Fiber design, fabrication, and evaluation

A new Raman gain fiber has been fabricated at University of Southampton to serve this project as well as other projects. The fiber with designation A1085-L10556 was paid with other ORC funds, from “Enhancing ORC/QLM International Collaborations”, to support the collaboration between ORC and IITM. The fiber is designed for cladding-pumping, and has an all-glass waveguiding structure comprising a P-doped inner cladding for guiding the pump and a Ge-doped core. It is hoped that this will result in higher Raman gain in the core than in the cladding, and thus promote SRS in the core over SRS in the cladding. Furthermore, the refractive index profile of the core is slightly ring-shaped with a central depression, which is compatible with the donut-shaped intensity profiles of OAMMs. Fig. 5 shows the refractive index profile and Fig. 6 shows the background loss of the fabricated Raman fiber.

The raised inner cladding has a diameter of $\sim 38 \mu\text{m}$ and the core has a diameter of $\sim 13 \mu\text{m}$. Thus, the area ratio is ~ 8.5 , which is compatible with high-efficiency SRS to the 1st Stokes order [9] (i.e., cascaded SRS can be avoided). Furthermore, the inner-cladding parameters are well-matched to high-energy pulse pumping with a YDF amplifier. Whereas the loss in Fig. 1 is on the high side ($\sim 15 \text{ dB/km}$ in the $1 - 1.1 \mu\text{m}$ range), it is still perfectly acceptable for expected device lengths of up to 20 m.

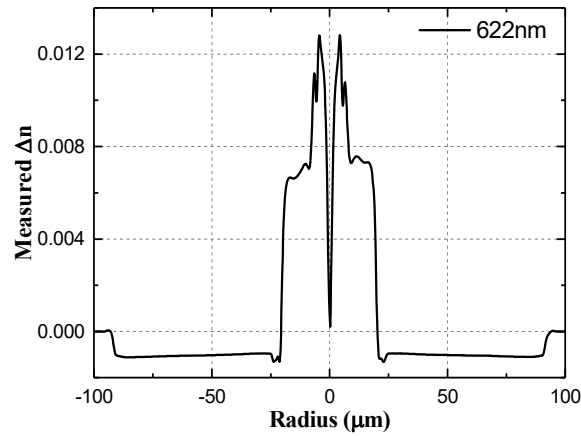


Figure 5. Measured refractive index profile of the double-clad fiber with ring-shape core (A1085-L10556).

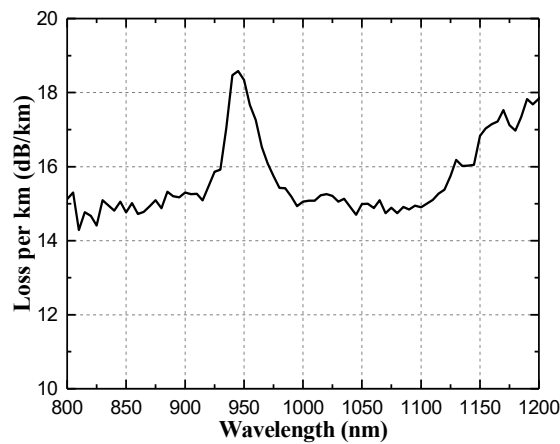


Figure 6. Measured background loss of the double-clad fiber with ring-shape core (A1085-L10556).

The core of the fiber supports OAMMs up to $|l| = 2$, where l is the topological charge. The mode splitting between different charges and the adjacent vector modes within the same linearly polarized (LP) mode group are shown in Fig. 7(a) and 7(b) respectively. The fiber dimension is optimized for maximum mode splitting permitted by the index profile of the preform. Compared with typical ring-core fibers whose refractive index difference between core and cladding being larger than 0.03, the fabricated fiber has a refractive index difference of ~ 0.015 , thus limiting the suppression of intermodal coupling. Nevertheless, for devices of $\sim 10\text{-m}$ length such coupling may be moderate.

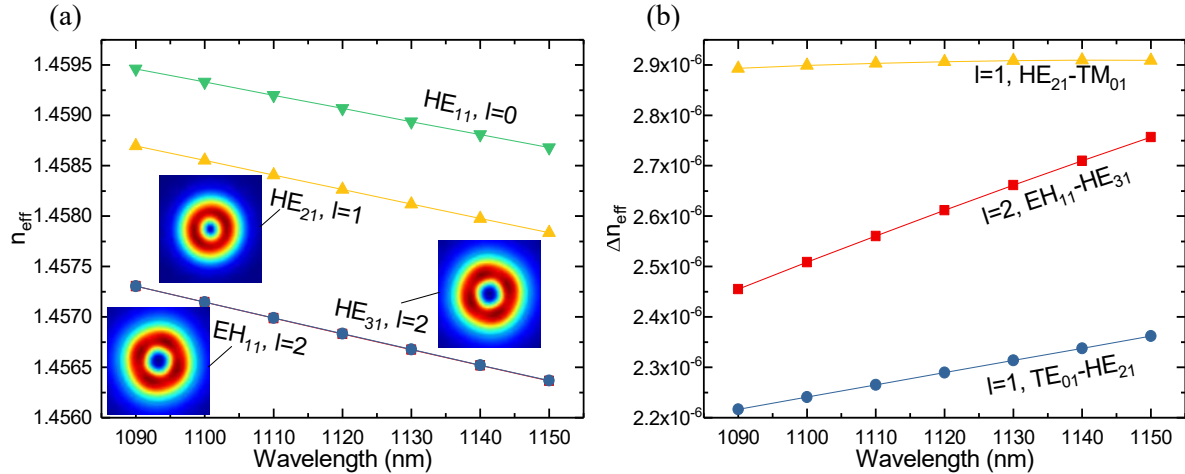


Figure 7. (a) Effective refractive indices for HE_{11} , HE_{21} , EH_{11} and HE_{31} modes vs wavelength. Insets show simulated mode field profiles. (b) Effective indices differences Δn_{eff} between the vector modes within the same LP mode group vs wavelength.

The fiber has not yet been tried for OAMM Raman amplification, but non-OAMM Raman laser operation has been demonstrated in another project [10].

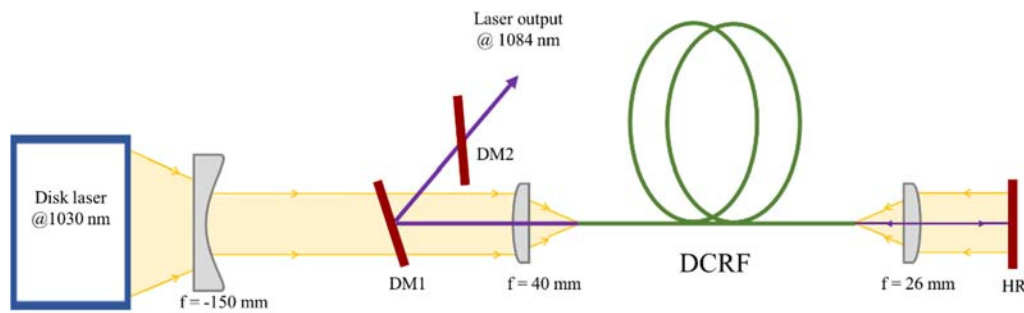


Figure 8. Experimental setup of the FRL. DM: dichroic mirror; HR: high-reflectivity mirror; (inset graph depicts the normalized RIP of the Raman fiber.)

The experimental configuration of the FRL is shown in Fig. 8. The length used in the experiment was 903 m, with an effective length of 277 m. The total signal round-trip loss is 40.9 dB. The pump source is a Yb:YAG disk laser (Trumpf HLD 4002) with up to 4 kW of continuous-wave (cw) or QCW output power at 1030 nm from a 200- μ m diameter, 0.1-NA core delivery fiber connected to a lens arrangement. We collimated the beam to a diameter of 30 mm and then passed it through an 18-mm aperture, which clips 42% of the power. This improves the beam parameter product (BPP) from 10 mm mrad (determined by the delivery fiber) to 6 mm mrad, so that it is better matched to the 2.9 mm mrad BPP of the DCRF's inner-cladding. This reduces the pump power not coupled into the inner cladding but into the outer cladding, where it can burn the coating. The overall pump launch efficiency was 30.8% from the disk laser into the inner cladding. The fiber had perpendicular cleaves in both ends. The fiber facet in the pump launch end served as a 4%-reflecting output coupler for the laser cavity. In the far end of the fiber, a high-reflectivity mirror with reflectivity $> 99\%$ for pump and signal close the laser cavity. Thus, the mirror reflects escaped pump back into the fiber in order to double-pass the pump.

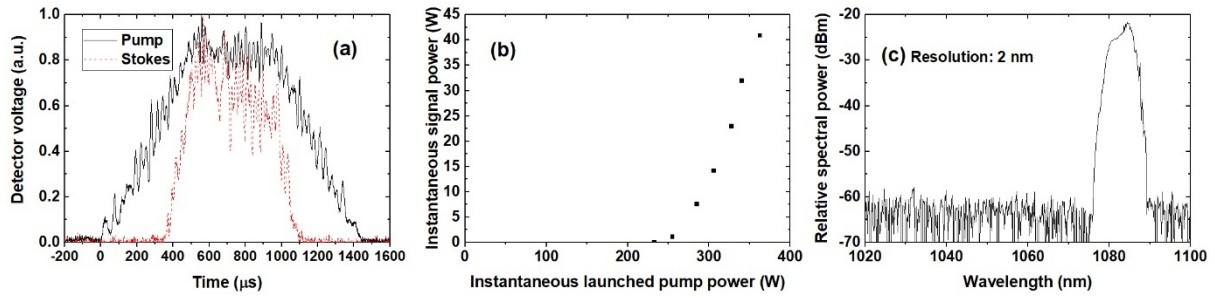


Figure 9. (a) Temporal traces of pump and Stokes pulses at maximum power (b) instantaneous signal power vs. instantaneous pump power launched into the inner cladding; (c) laser output spectrum at maximum power following spectral filtering in DM2.;

Despite these protective steps, the fiber still failed at the pump launch under cw operation. Therefore, we set the pump source to operate at 10 Hz with 1% duty cycle. This reduces the thermal load. Fig. 9 (a) shows the temporal traces of the pump and Stokes pulses at maximum pump power, which was 28 W (average) and 362 W (instantaneous) launched into the inner cladding. To evaluate the characteristics, we use the instantaneous power as averaged over the central 0.5 ms. Fig. 9 (b) shows the result. The threshold becomes 250 W, which agrees with simple estimates. The Stokes power then grows with 44% slope efficiency to 40 W at full power. A higher slope efficiency of 64% is achieved by cutting the fiber to 703 m to reach a maximum Stokes power of 46 W.

These results show that the FRL works largely as expected as it comes to threshold and efficiency (although the loss is on the high side). An interesting point here is that an area ratio of 8.5 may still be too large, according to other work of ours (this was subsequent to the fiber fabrication and was therefore not considered in the design of this fiber). Even though it may be possible to avoid (unwanted) cascaded SRS with that area ratio, this assumes a good pump–core overlap. However according to our simulations of Yb-doped fiber, this will not be the case in circular fibers with area ratio larger than 2.5, in the absence of mode-coupling [11]. This indicates that mode-coupling may be significant.

However, for amplification of an OAMM with high purity, it is necessary to excite and propagate the OAMM without mode-coupling. Furthermore, perturbations from circularity may mean that the fiber fails to support OAMMs. (This can be understood as if the constituent modes in the LP modal basis become non-degenerate¹ and thus beat as they propagate. In the OAMM basis this is equivalent to coupling between the left-hand and right-hand modes (although these are no longer true modes of the perturbed structure.) The beam quality was measured to $M^2 = 4.8$ at full power. This is higher than expected for a core V-value of 4.3 and mode-coupling, including coupling to cladding modes, and / or SRS in the inner cladding. Fig. 9 (c) shows the spectrum measured after DM2 at full power. The output peaks at 1084 nm, for a Raman shift of 484 cm^{-1} . This is larger than the germanosilicate value of $\sim 440 \text{ cm}^{-1}$ [12], and is closer to that of phosphosilicate [13]. This also indicates there is SRS in the inner cladding, or that P has diffused into the core. In the absence of diffusion, we estimate the Raman gain coefficient for unpolarized light to $1.03 \times 10^{-13} \text{ m/W}$ in the core (for germanosilicate [12]), and to $0.88 \times 10^{-13} \text{ m/W}$ in the inner cladding (for phosphosilicate, from [13]). This small difference suggests that other dopants such as Al_2O_3 may be better.

However, it is not clear to what extent these measurements with long fibers in the cw regime correlate with single-OAMM operation of pulsed amplifiers. These can be two orders of magnitude shorter, so the mode-coupling is expected to be much smaller. Low mode-coupling is a prerequisite for high-purity OAMM amplification, even though the interaction with the pump may get worse as a result of pump power in modes that don't interact well with the core. We have constructed a setup that can be

¹ In practice, the distinction is whether two modes are effectively degenerate, in the sense that the change in relative phase is small over the simulated length. Thus, the modes do not have to be strictly degenerate.

used for assessing mode stability. We plan to use this setup on this and / or other fibers and, if mode stability looks good, evaluate them as fiber Raman amplifiers for OAMMs.

Further discussion of simulations

We often use RP Fiber Power [14] for simulations. This software comprises several modules for different types of simulations. One module is based on the beam propagation method (BPM) with Fourier transformation in the diffractive step [15]. BPM is computation-intensive and is not necessarily the best choice (especially for longitudinally invariant structures). Furthermore, the implemented version makes use of the paraxial approximation and therefore solves the Fresnel equation rather than the Helmholtz equation. Furthermore, it is scalar rather than vectorial. However, it is convenient and we therefore still use it for some more sophisticated calculations, e.g., on the effect of local gain saturation on the modal gain in Yb-doped fibers. Note also that the eigenmodes of the Paraxial and Helmholtz equations are the same. The eigenvalues (i.e., propagation constants) are different, but are related by a simple formula [15]. However, we found several issues with BPM simulations of amplifiers, which are interesting but by and large unpublished, as far as we know. This has generated some uncertainty in the validity of the results and can also restrict the applicability. Here, we will outline some the issues.

In simulations of Yb-doped fiber amplifiers we always found longitudinal oscillations in the modal power calculated by RP Fiber Power, on the level of a few percent, and relatively rapid. One possible reason for this is the reference modes used in the overlap calculations for the determination of modal power. RP Fiber Power calculates the modes of a passive fiber structure (i.e., fiber modes), e.g., by direct numerical solution of the eigenmode equation or by using known analytical solutions (e.g., for step-index fibers). The errors in these will be very small. BPM discretizes the field on a relatively coarse grid (to make run-times acceptable) and also introduces a step length. Propagation of a single step of the field, from E_0 to E_1 , can formally be written as $E_1 = R/2 D R/2 E_0$.² Here, R represents the effect of the refractive index and D the effect of diffraction. The step is symmetrized by splitting R into two halves. R and D are linear operators and it follows that the overall propagator ($R/2 D R/2$) is also a linear operator. The linear operator supports modes (“BPM modes”), but these will differ somewhat from the actual fiber modes. Therefore, if we launch a fiber mode into the BPM solver then this will form a superposition of BPM modes. These will beat, and insofar as the modal power is evaluated in terms of the true fiber modes rather than the actual modes of the BPM solver (the BPM modes), the modal power will oscillate. This is a numerical effect that can mask actual physical effects that are our primary interest.

There are several possible ways to eliminate or reduce spurious numerical effects. One approach is to reduce the effect of the low sampling of the BPM grid. The grid can be made denser, but this may not be practical. In addition, a smoother refractive index difference works better than a step-index profile. For the latter, it only matters whether a grid point is inside or outside the core, which leads to large discretization effects and furthermore leads to a large artificial angular dependence in a circular fiber core. We verified that a smoothed profile reduced the modal power oscillations but did not eliminate them. See [6] for an example.

A second approach, which may seem more attractive, is to use the actual BPM modes for this. These are generally expected to be good approximations of the actual fiber modes. It is well-known that it is possible to extract the modes of the solver (i.e., the BPM modes) from a simulation [15]. We implemented this in Matlab. However, we focused on a different method for finding the BPM modes, namely, direct solution of the eigenmode equation $(R/2 D R/2) E = k E$, where E is an eigenmode and

² It is also straightforward to include amplification as a matrix multiplication. This may be nonlinear (e.g., locally saturating, in which case the matrix depends on the power level) or linear.

k is an eigenvalue³. This is discretized so the eigenmode will be an eigenvector. If the BPM grid comprises $M = N \times N$ points then the eigenvector E will have a length of N^2 . We note also that a discretized linear operator can always be cast in the form of a matrix multiplication. The refractive-index operator is in itself a matrix multiplication from start, so $R/2$ is a $M \times M$ matrix. (In fact, it is a diagonal matrix. Therefore, the matrix multiplication can be evaluated as an element-by-element multiplication of two vectors of length M .) The diffraction operator D is somewhat more complicated. In our case it is evaluated in the spatial-frequency domain, which involves Fourier transforms. The operator D is then split according to $F^{-1} M_D F$, where M_D is a $M \times M$ diagonal matrix with phase factors and F and F^{-1} are two-dimensional Fourier Transform (FT) and inverse FT, which convert the light field into, and out from, the spatial-frequency domain. M_D is applied as a simple matrix multiplication in the spatial-frequency domain while the FTs are generally evaluated with the fast Fourier Transform (FFT) algorithm (operation count famously scales as $N \log N$ in one dimension, and thus as $N^2 \log N$ and $M \log M$ in two dimensions). However, it is also possible to evaluate the FTs through matrix multiplication. The operation count scales as $M^2 \propto N^4$ so the FFT algorithm is normally preferred, but in our case, it allows us to write the diffraction operator as matrix multiplications according to $D = M_{IFT} M_D M_{FT}$, where M_{IFT} and M_{FT} are $M \times M$ matrices that perform the 2-D FTs through matrix multiplication. The BPM eigenvalue problem then becomes $E M_{BPM} = k E$, where the matrix $M_{BPM} = R/2 M_{IFT} M_D M_{FT} R/2$. The eigenvalue problem can then be solved directly through various methods (typically QR factorization) with built-in functions in Matlab, etc. We did this but had some issues with understanding the eigenvalues produced, as well as some of the modes. We were not able to use the results satisfactorily with RP Fiber Power's BPM module, for the launched and reference eigenmodes and propagation constants. One possible reason may be numerical inaccuracies. The QR factorization uses a numerical scheme which is subject to artefacts such as rounding errors. Perhaps a higher numerical precision would have produced better results, but QR factorization is computation-intensive. (It scales as $M^3 \propto N^6$ if the Householder algorithm is used. This may well be worse than that of BPM itself, depending on the number of propagation steps.)

We still expect that further work on the direct evaluation of BPM modes will resolve all the issues, and that this can be helpful for understanding various modal effects. However further massaging of parameters (notably refractive-index profile) allowed us to get satisfactory results with the problem we were working on at the time (higher-order Bessel-mode amplification [6], [7]).

Furthermore, we found additional effects of a more fundamental nature and shifted our focus to those. This also coincided with our shift in focus to optical angular momentum modes. One of the more fundamental aspects is that in the presence of a locally saturating nonlinearity, the power may actually oscillate between modes [16], [17].⁴ Furthermore, and of particular relevance to OAMM, is the numerical splitting of modes that are in reality degenerate. In a scalar treatment, OAMMs can be viewed as a superposition of two degenerate LP -modes, the so-called sine and cosine modes. Azimuthally, these are rotated with respect to each other by an angle $\pi/(2l)$, where l is the azimuthal mode order. In case of an OAMM, l is also the so-called charge of the mode. Furthermore, in case of an OAMM, the two LP -modes that can be viewed as the constituent LP -modes have equal amplitude and are longitudinally phase-shifted by $\pi/2$ with respect to each other. It is known that for the actual so-called vector-modes (i.e., with polarization), $l = \pm 1$ has certain special properties, e.g., as it comes to degeneracy [18]. Furthermore $l = \pm 1$ is generally undesired because the LP_{1m} -modes are split easily by bend-induced perturbations and fiber perturbations. This causes the phase-shift between the LP -

³ k is related to the modal propagation constant, but it is not the same. In the absence of gain and loss, the eigenvalues will have unit magnitude, while the propagation constant relates to the phase of the eigenvalue k , which is complex.

⁴ It may then be possible to redefine the modes, but such modes will be nonlinear and vary along the fiber, insofar as the power varies.

modes to deviate from $\pi/2$, which disrupts the propagation of the OAMM. (Alternatively, in the OAM mode basis, this can be understood as a coupling between the $l = +1$ and the $l = -1$ OAMM.)

Modes of higher azimuthal order (or charge) are more robust to bending, especially those of odd charge. Accordingly, our experimental work focused on charge 2 (we were not able to work with higher charge). We therefore focused our amplifier simulations (with BPM) on this case. However, we were not able to accurately propagate this OAMM even in the absence of amplification. We believe the reason for this is that the cosine and sine versions of the corresponding LP -mode, LP_{21} , are azimuthally rotated by $\pi/4$. FT-based BPM uses a rectilinear grid, in our case a square grid centered on the circular fiber core. Thus, if a symmetry axis of the cosine mode coincides with a coordinate axis, then the symmetry axis of the sine mode is at an angle of $\pi/4$ to that axis (i.e., on a diagonal, in case of a square grid). Then, these two modes will no longer be degenerate, which means the BPM solver does not support these OAMMs. That made it impossible for us to use BPM to study the impact of gain and gain saturation on the OAMM purity, and investigate and compare the amplification characteristics of Raman and Yb-doped fiber amplifiers, as we have done for other types of modes [6], [7]. It may be possible to generate meaningful results by adjusting the fiber parameters to make the sine and cosine modes perfectly degenerate, but this is not clear. For example, in case of amplifier simulations, it may be necessary for the BPM solver to support also other OAMMs, which generally suffer from the same splitting of constituent LP -modes. Intriguingly, the situation is different for $l = 1$. In this case, the symmetry axes of the cosine and sine modes are rotated by $\pi/2$, which mean that they both coincide with the coordinate axes and will be degenerate, in case of a circular fiber centered on a square grid.

Mode-selective gain saturation

Because of the problem of a rectangular grid, it may be necessary to use a modal approach for the simulation of mode-selective gain saturation and modal gain competition. This is by no means impossible. RP Fiber Power has a more conventional module (i.e., different from BPM), which can be used with actual fiber modes. However, this module is restricted to doped amplifiers based to stimulated emission, and it cannot handle Raman amplifiers. On the other hand, in another project, we have developed a similar model for Raman amplifiers.

Both the RP Fiber power module and our Raman model are used for a HOM (LP_{08} , i.e., not an OAMM) in [7]. They both assume the pump and signal are incoherent. By contrast, our BPM calculations assume both the pump and signal are coherent. In reality, the pump is likely to be incoherent. However, since the pump power is distributed over many modes with a wide range of propagation constants, even a pump that is mathematically (and strictly) coherent will in practice be incoherent. Even though the phase relations between the different pump modes are constant in time (because they are coherent), they are still random relative to each other. In our BPM simulations, we typically assume that all modes are excited with equal power and random phase at the launch (and the relative phases remain random throughout the fiber). The deviations of the local intensity when many modes with random phase are added from the average value (as obtained within incoherent pumping) is likely to be insignificant.

As it comes to the signal, this will be coherent to a larger or lesser degree. This matters when there are several signal modes, which can beat. We are generally interested in single-mode operation of a multimode amplifier (i.e., which supports several signal modes), and the MM amplifier is seeded by a single-mode source with perfect spatial coherence at the launch point. Consider first the case of high temporal coherence. This means that the difference in effective index between modes is small enough for the spatial coherence to be maintained throughout the fiber, and thus that a spatial interference pattern stays constant in time. For example, if $\Delta n_{eff} = 10^{-4}$ (the average value between scalar modes at $1.1 \mu\text{m}$ in a $41\text{-}\mu\text{m}$ diameter core), then in a 10-m amplifier, two neighboring modes typically walk off by 1 mm. (This assumes that the modes are not exchanging energy and furthermore that the average

difference in group index is similar to that of the effective index. This is reasonable, although the average difference in group index is normally smaller, and can be much smaller.) If the coherence length exceeds 1 mm then neighboring modes can be considered coherent. This corresponds to a linewidth of 2.60 nm (644 GHz) at 1.1 μm . If the overall spread in (group) index is 10^{-3} , then all modes are coherent over 10 m if the linewidth is 0.26 nm or less.

For larger linewidths the coherence degrades along the fiber. (More precisely, the phase relations in any point of the fiber only remain approximately constant over a limited distance from that point.) For sufficiently large linewidths the coherence may degrade sufficiently rapidly to make it negligible for most modes. However degenerate cosine and sine modes, and thus the corresponding clockwise (CW) and counter-clockwise (CCW) OAMMs, are always mutually coherent, irrespective of linewidth. Furthermore, in our experiments on single-OAMM fiber Raman amplification, we found the interaction with the degenerate CCW mode to be most significant [4], [5]. Therefore, it seems necessary to consider coherent effects.

By contrast, when amplifying a mode with $l = 0$ (the fundamental mode or a HOM), there is no mode which is perfectly degenerate with the target mode. Incoherent simulations may then be most relevant, at least for large signal linewidths. There may still be a spurious quasi-degeneracy with some mode, which may be unknown *a priori*, and can lead to unexpected effects. We also mention that the group velocity of such spuriously quasi-degenerate modes will generally be different. In principle, this means that the linewidth matters, but if the walk-off is small this may not be significant. Interestingly for a HOM (LP_{08} , i.e., not an OAMM) the difference between coherent simulations in [6] and incoherent ones in [7] are quite larger for the YDFA, but small for the FRA.

Although we have yet to develop or acquire software for coherent simulations of OAMM amplification, we can still draw some conclusions. The gain saturation (including mode-selective gain saturation) can be local (when the local gain depends on the local signal intensity). This is the case with conventional stimulated emission (from an excited population), but not with Raman amplification. However, there is also non-local gain saturation. This depends on how the signal depletes the pump along the fiber, and thus influences the local pump intensity. The local pump intensity influences the local gain even when the local signal intensity doesn't. This saturation is non-local because it depends on how the pump has propagated up to a certain location, rather than on what happens in that location. If the pump depletion varies across the fiber as a result of the transverse signal distribution, then the non-local gain saturation will be mode-selective (as is the local gain saturation).

In addition to the type of gain (with or without local gain saturation), the gain saturation and its mode selectivity also depends on the coherence of the signal. Although the coherent case seems most relevant (at least for OAMMs), it is useful to first consider the simpler and more widely studied incoherent case. Incoherent gain saturation (of modes) depends on the modal intensity distribution. The modal self-saturation is then always larger than the modal cross-saturation of the gain. The exception to this is for modes with identical intensity distributions, which is the case for a matched pair of OAMMs. Thus, for such a pair, the incoherent modal self-saturation and cross-saturation will be the same. In contrast to modes with $l = 0$ [7], it is not clear if the absence of local saturation in a FRA helps to preserve the mode purity of an OAMM, when the dominant purity degradation is to the matched OAMM with opposite charge.

Furthermore, as already stated, gain saturation effects between such degenerate modes is coherent rather than incoherent. This modifies the saturation [16]. When two modes interact, the saturation of the mode with less power increases relative to the saturation of the mode with more power. In case of modes with different intensity distributions, the self-saturation may still be larger than the cross-saturation. However, in case of mode with the same intensity distribution, the saturation of the mode with more power (typically a desired mode) will be smaller than the mode with lower power. This has

been studied thoroughly in the context of gain-gratings formed by counter-propagating waves in a single-mode fiber (e.g., [19]). When the objective is to amplify a single mode, the weaker-power modes are generally parasitic, so coherent gain saturation is beneficial.

We are not aware of any exhaustive study of the difference between coherent gain saturation depending on type of mode and type of gain medium. We note however that the coherence matters for the local as well as the non-local gain saturation. Consider a matched pair of OAMMs where most of the power is in the desired CW mode. To be specific, assume that these modes correspond to the LP_{21} -mode. Instead of considering the power to be distributed between the CW and CCW mode, it is possible to consider it to be distributed between the CW mode and one of the LP -modes, say, the cosine mode (even though these refer to different modal bases). The more power is transferred from the high-power CW mode the more peaked the signal intensity distribution will be. This will affect any local as well as non-local mode-selective gain saturation. The sine mode overlaps better with the high-gain regions and will therefore see a higher relative gain. This decreases the azimuthal variation of the signal intensity, i.e., increases the power in the desired CW mode for gain media with non-local mode-selective gain saturation, even in the absence of local gain saturation. However, it seems likely that with local gain saturation, the effect will be larger and thus more beneficial.

To summarize this section, we have outlined and discussed issues related to mode-selective gain saturation (and thus modal gain competition) of OAMMs. We note there are several different regimes, viz.:

- Coherent vs. incoherent modes (or more generally, degree of coherence) and related to this, coherent gain competition
- Non-degenerate vs. degenerate modes (including quasi-degenerate modes)
- Modes with perfect (high) or low intensity overlap
- Gain media with and without local gain saturation

We emphasize that the perfect degeneracy and signal intensity overlap are distinguishing properties of matched pairs of OAMMs. These are important for mode-selective gain saturation. Because of the degeneracy, the gain-saturation can be assumed coherent, and in case of perfect intensity overlap, this favors a stronger mode over a weaker one. There are likely to be significant differences between Raman and Yb amplification because of the difference in local gain saturation. Whereas a gain medium without local gain saturation may be preferable for LP_{0m} -modes, local gain saturation helps to suppress (unwanted) coupling from a desired OAMM to the matched OAMM of opposite charge. We also reiterate that we have not considered polarization effects. Orthogonal polarizations do not interfere so will not interact through coherent mode competition.

Interactions, transitions, meetings

Many of these meetings were not funded by this project but nevertheless offered opportunities to talk to project partners and present project results to interested parties in the DoD.

IIT Madras, September 2016

Visit, J. Nilsson, 17 days as part of GIAN (Indian government) lecture course.

Discussions with project partners.

SPIE Photonics West, San Francisco, CA, February 2017

J. Nilsson

Interaction with project partners and DoD personnel.

Visit to IITM, March 2017, in relation to the UK Engineering and Physical Sciences Research Council Global Research Challenge

J. Nilsson, D. Payne, J. Sahu

Discussions with project partners.

Visit to Lincoln Laboratories, April 24 2017

J. Nilsson

Presentation of project results.

Visit to Army Research Laboratories, April 25 2017

J. Nilsson

Presentation of project results.

Visit to Navy Research Laboratories, April 28 2017

J. Nilsson

Presentation of project results.

Visit by Nathaniel Lockwood, AFOSR/EOARD program manager, May 30 2017

Discussions and presentations

Visit by Scott Robertson, AFOSR/AOARD program manager, Sept 15 2017

Project review

Advanced Solid State Lasers conference Nagoya, Japan Oct 1-5 2017

Johan Nilsson, Sheng Zhu

Presentation of project results [3], [6]

Project discussions with Briana Singleton (AFOSR/AOARD program manager) and Balaji Srinivasan (IITM PI).

Visit to Navy Research Laboratories, April 20 2018

J. Nilsson

Presentation of project results.

Conference on Lasers and Electro-Optics Pacific Rim, Hong Kong, July 29 – Aug 3 2018

J. Nilsson

Tutorial presentation, which included project results.

EuroPhoton conference, Barcelona, Spain, Sept 2 – 7 2018

J. Nilsson

Summer school lecture, which included project results

Meetings with Nathaniel Lockwood, AFOSR/EOARD

Telephone conference with Brian Anderson, Angel Flores, and Anthony Hostutler (AFRL), and Nathaniel Lockwood, AFOSR/EOARD.

Meeting with Mark Dubinskii, ARL

Conclusions, discussion, and possible future work

As discussed already, there are plenty of interesting possible work in the area of mode-selective gain saturation in gain media with and without local gain saturation, for different types of modes. There are no further points at present.

Honors and awards

Johan Nilsson became a Fellow of the SPIE.

Contributing staff, students, and visitors, University of Southampton

Johan Nilsson, PI

David Payne, co-I

Jayanta Sahu, co-I

Peter Kazansky

Yutong Feng

Shankar Pidishety, initially visiting academic from IIT Madras, later member of ORC staff

Pranabesh Barua, fiber fabrication

Achar V. Harish, PhD student

Soonki Hong, PhD student

Sheng Zhu, PhD student

Siddharth Ramachandran, visiting academic

Balaji Srinivasan, visiting academic from IIT Madras (also IIT Madras PI)

Pengling Yang, visiting academic

Yusuf Panbiharwala, visiting student from IIT Madras (also participating in project at IIT Madras)

Investigators, IIT Madras

Balaji Srinivasan, PI

Deepa Venkitesh, co-I

Anil Prabhakar, co-I

References

(*) designates full or part funding by this grant (FA2386-16-1-0005).

1. Q. Kang, P. Gregg, Y. Jung, E. L. Lim, S. Alam, S. Ramachandran, and D. J. Richardson, "Amplification of 12 OAM Modes in an air-core erbium doped fiber," *Optics Express* **23**, 28341 (2015).
2. Y. Jung, Q. Kang, R. Sidharthan, D. Ho, S. Yoo, P. Gregg, S. Ramachandran, S.-U. Alam, and D. J. Richardson, "Optical Orbital Angular Momentum Amplifier Based on an Air-Hole Erbium-Doped Fiber," *J. Lightwave Technol.* **35**, 430–436 (2017).
3. (*) Shankar Pidishety, Sheng Zhu, Peter G. Kazansky, Johan Nilsson and Balaji Srinivasan, "Amplification of orbital angular momentum beam in a fiber Raman amplifier," in *Laser Applications Conference 2017*, OSA Technical Digest (online) (Optical Society of America, 2017) paper JTh2A.6.
4. (*) Sheng Zhu, Shankar Pidishety and Johan Nilsson, "15-dB Raman amplification of an optical orbital angular momentum mode in a step-index fiber", in *Advanced Solid State Lasers 2018*, OSA Technical Digest (online) (Optical Society of America, 2018), paper AW2A.4
5. (*) Shankar Pidishety, Sheng Zhu, Yutong Feng, Balaji Srinivasan, and Johan Nilsson, "Raman amplification of optical beam carrying orbital angular momentum in a multimode step-index fiber", submitted
6. (*) Sheng Zhu, Shankar Pidishety, Yutong Feng, Jeff Demas, Siddharth Ramachandran, Balaji Srinivasan, and Johan Nilsson, "Multimode Raman pumping for power-scaling of large area higher order modes in fiber amplifiers", in *Advanced Solid State Lasers 2017*, OSA Technical Digest (online) (Optical Society of America, 2017), paper ATh4A.4
7. (*) Sheng Zhu, Shankar Pidishety, Yutong Feng, Soonki Hong, Jeff Demas, Raghuraman Sidharthan, Seongwoo Yoo, Siddharth Ramachandran, Balaji Srinivasan, and Johan Nilsson, "Multimode-pumped Raman amplification of a higher order mode in a large mode area fiber", *Opt. Express* **26**, 23295-23304 (2018)
8. M. Beresna, M. Gecevičius, P. G. Kazansky, and T. Gertus, "Radially polarized optical vortex converter created by femtosecond laser nanostructuring of glass", *Appl. Phys. Lett.* **98**, 2011.
9. J. Ji, C. A. Codemard, M. Ibsen, J. K. Sahu, and J. Nilsson, "Analysis of the conversion to the 1st Stokes in cladding-pumped fiber Raman amplifiers", *IEEE J. Sel. Top. Quantum Electron.* **15**, 129 – 139 (2009)
10. Y. Feng, S. Zhu, S. Hong, H. Lin, P. Barua, J. Sahu, and J. Nilsson, "Spatially Gain-Tailored Fiber Raman Laser Cladding-Pumped by Multimode Disk Laser at 1030 nm," in *Conference on Lasers and Electro-Optics*, OSA Technical Digest (online) (Optical Society of America, 2018), paper JTh2A.109.
11. Yutong Feng, Pablo G. Rojas Hernández, Sheng Zhu, Ji Wang, Yujun Feng, Huaiqin Lin, Oscar Nilsson, Jiang Sun, and Johan Nilsson, "Pump absorption, laser amplification, and effective length in double-clad ytterbium-doped fibers with small area ratio", submitted
12. S. T. Davey, D. L. Williams, B. J. Ainslie, W. J. M. Rothwell, and B. Wakefield, "Optical gain spectrum of GeO₂-SiO₂ Raman fibre amplifiers," *IEE Proc. J - Optoelectron.* **136**, 301–306 (1989).
13. Evgeny M. Dianov, "Advances in Raman Fibers," *J. Lightwave Technol.* **20**, 1457-1462 (2002).
14. R. Paschotta, "Modeling of ultrashort pulse amplification with gain saturation," *Opt. Express*, vol. 25, no. 16, p. 19112, 2017.
15. M. D. Feit and J. A. Fleck, "Computation of mode properties in optical fiber waveguides by a propagating beam method," *Appl. Opt.* **19**, 1154 (1980).

16. D. Vysotsky and A. Napartovich, "Mode competition in steady-state optical waveguide amplifiers," J. Exp. Theor. Phys. **108**, 547–556 (2009).
17. Arlee V. Smith and Jesse J. Smith, "Mode competition in high power fiber amplifiers," Opt. Express **19**, 11318-11329 (2011)
18. Siddharth Ramachandran, in various discussions and presentations
19. Serguei Stepanov, "Dynamic population gratings in rare-earth-doped optical fibres", J. Phys. D: Appl. Phys. **41** 224002 (2008)

Additional publications

Additional publications with full or part funding by this grant (FA2386-16-1-0005).

Yusuf Panbiharwala, Pengling Yang, Johan Nilsson, and Balaji Srinivasan, "Design and demonstration of an all-fiber tandem pumped master oscillator power amplifier", in Proc. International Conference on Fibre Optics and Photonics 2016 (Optical Society of America, 2016), Tu2E.3

A. V. Harish and J. Nilsson, "Optimized modulation formats for suppression of stimulated Brillouin scattering in optical fiber amplifiers," in 2017 European Conference on Lasers and Electro-Optics and European Quantum Electronics Conference, (Optical Society of America, 2017), paper CJ_P_29.

Y. Panbiharwala, A. Ghosh, J. Nilsson, D. Venkitesh, and B. Srinivasan, "Experimental investigation of the onset of modulation instability as a precursor for the stimulated Brillouin scattering in Yb-doped fiber amplifiers", in Fiber Lasers XV: Technology and Systems, I. Hartl and A. L. Carter, Eds, Proc. SPIE vol. 10512, 105122X (2018)

A. V. Harish and J. Nilsson, "Optimization of phase modulation formats for suppression of stimulated Brillouin scattering in optical fibers", IEEE J. Sel. Top. Quantum Electron. **24**, 5100110 (2018)